Development of an Improved Analytical Model for the NASA/JPL 70-Meter Antenna Hydraulic Servovalve

E. A. Carrell and R. E. Hill
Ground Antennas and Facilities Engineering Section

A new mathematical model for the hydraulic servovalve employed in the axis servos of the DSS 14 70-m antenna is described. The model is based on a system of simultaneous nonlinear equations relating pressure and flow in the multiple orifices and internal flow paths of the valve. The model accounts for critical imperfections expected to affect valve performance such as overlap, radial leakage clearance, and rounded orifice edges attributed to mechanical wear. The model is structured for use with mathematical analysis software and execution on 80286-based microcomputers. It is expected to provide a new insight into the pressure and flow responses of the valve in the region of zero flow.

I. Introduction

The recent upgrades of the 70-m antenna controllers and axis-positioning servos have led to a sustained use of automated capabilities of the pointing system. This increased use, in turn, has elevated axis drive-torque duty factors and has raised concerns about excessive mechanical wear of drive motors, gear reducers, and other drive components. At the same time, the pointing requirements for the X-band (8.4-GHz) frequency 70-m aperture antenna and the expectation of future K-band (32-GHz) capability dictate an improved level of axis-servo performance. The servo-design task thus requires the optimization of servo-pointing performance and minimization of a drive-torque wear factor. In this regard, the servo properties of the hydraulic servovalves, which control the flow to the axis drive motors, are of critical importance.

The servovalve must have sufficient flow capacity to accommodate slew antenna motion at its maximum stroke, yet it must provide slow, accurate antenna motion for tracking near its null or zero-flow position. Thus, the critical function of the valve, which is to accurately control antenna axis pointing at the low-tracking velocity, requires the valve to operate around its null region. Furthermore, the resistance to pointing errors caused by external disturbance torques is proportional to the nonlinear change in pressure with flow at the valve orifices in their null region [1]. For these reasons, an accurate model of valve operation in the null region is crucial to system analysis, behavior prediction, and pointing improvement.

In the presently employed conventional servovalve model, the four valve orifices are simplified into one equivalent orifice, with varying area, in a piecewise linearization of the orifice equation [2]. For practical valve applications, nonlinear effects become significant only when the valve is operated in its null region or at very large load pressures. This approximation is sufficient only for high-flow or low-load pressure operation but can be inaccurate at extreme low-flow conditions. Therefore, a mathematical computer

model of the servovalve is being created, in conjunction with actual test data, to be used for valve performance prediction, focusing particular attention on the null region operation. This analysis enables the prediction of antenna pointing based upon measurable valve parameters.

The complete servovalve modeling project consists of three phases. First, a detailed analytical computer model of the servovalve is created, based upon equations describing the pressure and flow relationships in the presence of mechanical imperfections. Next, simulation is performed using this model, and the results are compared with both the manufacturer's data and similar tests performed on the valve in a hydraulic test-bench setting. This simulator is refined until these results are in close agreement or the discrepancies are explained. Finally, to evaluate the effects that imperfections have on valve behavior, a sensitivity analysis is conducted by varying the parameters in the computer simulation and determining the influence these variations have on valve performance.

The following discussion presents current progress on the first project phase, that of developing the model. The fundamental flow relationships that form the basis of the model are presented and solved for a typical set of conditions. Critical components of these equations, including the orifice-area calculation and the characterization of the discharge coefficient, are analyzed in detail. The discussion concludes with a brief description of plans for completing the model and satisfying the final two phases of the project, which include verifying the model and simulating the valve for parameter sensitivity testing.

II. Fundamental Flow Relationships

The model is based in MATLAB[1] software, which is used to solve the system of nonlinear pressure–flow relationships given in Eqs. (1)–(7). The orifice equation, Eqs. (1)–(4), describes flow at each of the four individual sets of valve supply and return ports. Figure 1 gives a schematic of the internal function of the valve for reference; dimensions are exaggerated for clarity.

$$Q_{R1} = C_d A_o \sqrt{\frac{2}{\rho}(P_{L1} - P_R)} \tag{1}$$

$$Q_{R2} = C_d A_c \sqrt{\frac{2}{\rho}(P_{L2} - P_R)} \tag{2}$$

$$Q_{S1} = C_d A_c \sqrt{\frac{2}{\rho}(P_S - P_{L1})} \tag{3}$$

$$Q_{S2} = C_d A_o \sqrt{\frac{2}{\rho}(P_S - P_{L2})} \tag{4}$$

$$Q_{R1} + Q_{S1} + Q_{R2} + Q_{S2} = 0 \tag{5}$$

$$Q_{R2} + Q_{S2} + Q_{L2} = 0 \tag{6}$$

$$Q_{L1} + Q_{L2} = 0 \tag{7}$$

$$P_{L2} - P_{L1} = 0 \tag{8}$$

where

A_c = area of a closing orifice

A_o = area of an opening orifice

C_d = discharge coefficient

P_{L1} = pressure at load port No. 1

P_{L2} = pressure at load port No. 2

P_R = return pressure

P_S = supply pressure

Q_{L1} = flow through load port No. 1

Q_{L2} = flow through load port No. 2

Q_{R1} = flow through return port No. 1

Q_{R2} = flow through return port No. 2

Q_{S1} = flow through supply port No. 1

Q_{S2} = flow through supply port No. 2

ρ = hydraulic fluid density

The four port flows are related to the load flows by continuity, Eqs. (5)–(7). The solution of this set of equations yields the seven flows for a given current-input and differential-load pressure condition. Equation (8) provides a no-load condition, which is a standard test case, by restricting the load pressure drop to zero. The system of equations was solved with a supply pressure of 3000 psi, and the results are given in Fig. 2. This no-load flow is an example of a typical valve simulation that can be compared with equivalent plots from actual valve tests.

Alternatively, load pressures can be determined from the set of equations, given a current input and a load-flow constraint. A blocked port condition in which there is no

[1] MATLAB is a registered trademark of the Math Works, Inc., South Natick, Massachusetts, 1989.

flow through the load ports is invoked when Eqs. (6)-(8) are replaced with

$$Q_{R2} + Q_{S2} + Q_{Le} = 0 \tag{9}$$

$$Q_{Le} = K(P_{L1} - P_{L2}) \tag{10}$$

where

Q_{Le} = leakage flow between load ports resulting from radial clearance between spool and sleeve

K = constant describing flow between concentric pipes

This system of equations, Eqs. (1)-(5) and (9)-(10), was solved for the pressure drop across the load ports, which is a standard test condition to show the pressure gain. The results are given in Fig. 3. This pressure gain plot gives another example of a typical valve simulation that can be compared with equivalent plots from actual valve tests.

III. Valve-Orifice Areas

Correct representation of the change in the valve-orifice area with spool displacement is crucial to revealing many nonlinear effects through the orifice equation. Three important parameters that affect orifice flow during operation near null are the radial leakage clearance between the spool lands and the sleeve, the rounded orifice edges that result from mechanical wear, and the valve overlap. Radial leakage clearance refers to the radial gap between the lands, which are sections of the spool having a larger diameter, and the sleeve, or bushing in which the spool rides, as indicated by C_r in Fig. 1. This clearance allows flow between the supply and return ports at all times. Because each spool and sleeve is machined as a matched pair, radial clearance is a controlled parameter.

The sharp corners of both the spool lands and the sleeve ports that form the orifices become rounded by wear. The wear process is enhanced by the use of contaminated hydraulic fluid. Sharp corners are crucial for producing flow that can be described by familiar, simple equations. Once corners become rounded, parameters of the flow equations take on a new form. The orifice area is slightly increased by an amount that becomes significant for small orifices that result from operation in the null region, thereby increasing the effective Reynolds number in this region. The discharge coefficient changes for the low Reynolds numbers that occur around null. This relation will be discussed in Section IV.

Valve overlap refers to the length of the land being extended such that at null, the port is not completely closed. Underlap refers to the companion condition in which the land length is undersized such that the port remains completely closed for spool displacements off null that are less than the length of underlap. Thus, small displacements off null of an underlapped spool have no effect on flow, thereby defining a dead zone.

The valve-orifice area is calculated from the dimensions indicated in the magnified orifices of Fig. 1. The port in the sleeve is round, having a diameter D_p. Its uncovered area is found by integrating the semicircle twice, as shown in Fig. 4.

$$\text{Area} = 2 \int \sqrt{r^2 - x^2}\, dx \tag{11}$$

In consideration of worn ports, the r, which represents the radius of the port, is $D_{po}/2 + l_{po}$, where l_{po} is a dimension that results from wear. For a port that opens with a positive spool displacement, the limits of integration are from $-D_{po}/2 - l_{po}$ to $-D_{po}/2 - l_{po} + l_{vo}$. Replacing r with b_o in Eq. (11) and integrating between the limits gives

$$A_{vo} = (-b_o + l_{vo})\left[b_o^2 - (-b_o + l_{vo})^2\right]^{1/2} + b_o^2 \cdot \sin^{-1}\left(\frac{-b_o + l_{vo}}{b_o}\right) + \frac{\pi b_o^2}{2} \tag{12}$$

where, as shown in Fig. 1

$$\begin{aligned} l_{po} &= r_{po} - r_{po}\cos\theta_o \\ l_{so} &= r_{so} - r_{so}\cos\theta_o \end{aligned} \tag{13}$$

and

$$\theta_o = \tan^{-1}\left(\frac{C_r + r_{po} + r_{so}}{|X_v - O_{vo} + r_{po} + r_{so}|}\right) \tag{14}$$

and, as shown in Fig. 4

$$b_o = D_{po}/2 + l_{po} \tag{15}$$

$$l_{vo} = X_v - O_{vo} + l_{po} + l_{so} \tag{16}$$

The total orifice area is

$$A_o = \frac{A_{vo}}{\cos\theta_o} \tag{17}$$

The parameters at a port that opens with positive spool displacement are

O_{vo} = valve overlap

r_{so} = radius of curvature of the spool land edge

r_{po} = radius of curvature of the edge of a sleeve

X_v = spool displacement from null

For a port that closes with a positive spool displacement, the equations are complementary. The limits of integration of Eq. (2) become $D_{pc}/2 + l_{pc} - l_{vc}$ to $D_{pc}/2 + l_{pc}$. Replacing r with b_c in Eq. (11) and integrating between the limits for a closing orifice gives

$$A_{vc} = -(b_c - l_{vc})\left[b_c^2 - (b_c - l_{vc})^2\right]^{1/2} - b_c^2 \sin^{-1}\left(\frac{-b_c - l_{vc}}{b_c}\right) + \frac{\pi b_c^2}{2} \tag{18}$$

where, as shown in Fig. 1

$$\begin{aligned} l_{pc} &= r_{pc} - r_{pc}\cos\theta_o \\ l_{sc} &= r_{sc} - r_{sc}\cos\theta_o \end{aligned} \tag{19}$$

and

$$\theta_c = \tan^{-1}\left(\frac{C_r + r_{pc} + r_{sc}}{|X_v + O_{vc} - r_{pc} - r_{sc}|}\right) \tag{20}$$

and, as shown in Fig. 4

$$b_c = \frac{D_{pc}}{2} + l_{pc} \tag{21}$$

$$l_{vc} = |X_v + O_{vc} - l_{pc} - l_{sc}| \tag{22}$$

Finally, the total orifice area is

$$A_c = \frac{A_{vc}}{\cos\theta_c} \tag{23}$$

Parameters for a port that closes with positive spool displacement are

O_{vc} = valve overlap

r_{sc} = radius of curvature of the spool land edge

r_{pc} = radius of curvature of the edge of a sleeve

The total orifice areas, A_o and A_c, are given in Eqs. (17) and (23) and are used in the orifice equation, Eqs. (1)–(4), to relate valve-orifice flow to the pressure drop across the orifice. The spool displacement from null, X_v, is assumed to be linearly proportional to valve input current.

IV. Discharge Coefficient

As mentioned previously, the other component of the orifice equation that contains nonlinearities for null-region operation is the discharge coefficient, C_d. For turbulent orifice flow, C_d is constant at 0.611 [3,4]. However, for laminar flow, C_d can be approximated as proportional to the square root of the Reynolds number, as demonstrated by the plot in Fig. 5 [3]. The slope of this relation is defined by a parameter labeled delta, which is dependent upon the critical Re for which the orifice flow changes from laminar to turbulent. Both the valve radial clearance and the rounding of port edges act to increase orifice area and decrease the Reynolds numbers, causing flow to remain laminar for larger spool displacements. The critical Re is dependent also upon the rounding of port edges, which strengthens the tendency of the orifice flow to form a boundary layer and remain laminar [4].

Present effort is directed toward modeling the change in C_d with Re in a piecewise linear manner. Flow is dependent upon C_d, which is dependent upon Re, which is dependent on flow. This interdependency suggests a need for an iterative process to solve for the parameters simultaneously. Current analysis reveals that when the ratio of spool displacement, X_v, to the average of spool and port wear radius of curvature, $1/2(r_p + r_s)$, is less than or equal to 10, δ reaches its asymptotic value of 0.2, which corresponds to a critical Reynolds number of 9.3. Preliminary simulation needs to be conducted according to this assumption unless field tests prove the assumption to be false.

V. Summary

Current progress on the development of a nonlinear model of the servovalve that controls the DSS 14 70-m antenna has been described. The model is based on equations that characterize valve-orifice flow and account for critical flaws through a detailed orifice-area analysis. The

examined imperfections that affect valve performance include rounded orifice edges that result from wear, valve overlap, and radial leakage clearance. The effects these flaws have on the discharge coefficient were described. Also, an exemplary simulation based on the analysis was provided for the no-load-differential pressure condition. Steps for completing and validating the model and using it to simulate the valve for parameter sensitivity testing follow.

The equations that have been derived to this point describe flow through an open port. However, orifice flow is no longer a valid assumption once the sleeve port is completely covered by the spool land. The flow through such a closed port is restricted to the leakage allowed by the radial clearance, as referred to earlier. Equations to properly characterize this flow must be included in the final model. A graduated combination of orifice and parallel plate flow is a possibility.

Other nonlinearities to be addressed include deadband and hysteresis. Deadband results either from valve overlap or from discontinuous spool motion, or from a combination of both. Hysteresis is a consequence of friction and mechanical backlash that prevent monotonic spool motion. Piecewise linear functions of input current with flow are candidates for both deadband and hysteresis models.

Fluid parameters, including density, viscosity, and content of additives, have been determined by testing samples of the fluid from the operating antenna. At present, other parameters are estimated. Mechanical dimensions are estimated by examining drawings from the valve manufacturer, Moog Inc., and a Jet Propulsion Laboratory drawing. Other dimensions are given directly in Moog's valve catalog [5]. Valve dimensions need to be confirmed by disassembling the valve and measuring the dimensions of its internal components after experiments have been conducted.

The validity of the model needs to be demonstrated by checking its consistency through tests conducted on the valve on a hydraulic test bench. The measurements should include the relationships among closed-load-port flow, no-load-differential pressure, leakage flow, and input current with spools of varying dimensions simulating wear. The complete model that accurately predicts valve performance within a reasonable error needs to be compared systematically to the existing linearized model to determine its relative consistency with field test data.

Upon completion of the project, simple simulations could be run on a computer model for a quick estimation of the effects a specific parameter has on servovalve performance. This detailed mathematical servovalve model is expected to increase the accuracy of antenna axis servopointing prediction by replacing the conventional servovalve model in a simulation of the entire antenna servo system.

Acknowledgment

The authors express gratitude to L. Alvarez for his comments on and discussion of the first draft of this article.

References

[1] R. E. Hill, "Disturbance Torque Rejection Properties of the NASA/JPL 70-Meter Antenna Axis Servos," *TDA Progress Report 42-99*, vol. July–September 1987, Jet Propulsion Laboratory, Pasadena, California, pp. 170–179, November 15, 1989.

[2] R. E. Hill, "Dynamic Models for Simulation of the 70-M Antenna Axis Servos," *TDA Progress Report 42-95*, vol. July–September 1988, Jet Propulsion Laboratory, Pasadena, California, pp. 32–50, November 15, 1988.

[3] H. E. Merritt, *Hydraulic Control Systems*, New York: John Wiley & Sons, Inc., 1967.

[4] T. J. Viersma, "Investigations into the Accuracy of Hydraulic Servomotors," *Philips Research Reports 16*, pp. 528–534, 1961.

[5] W. J. Thayer, "Transfer Functions for Moog Servovalves," Technical Bulletin 103, Moog Inc., East Aurora, New York, Rev. 1965.

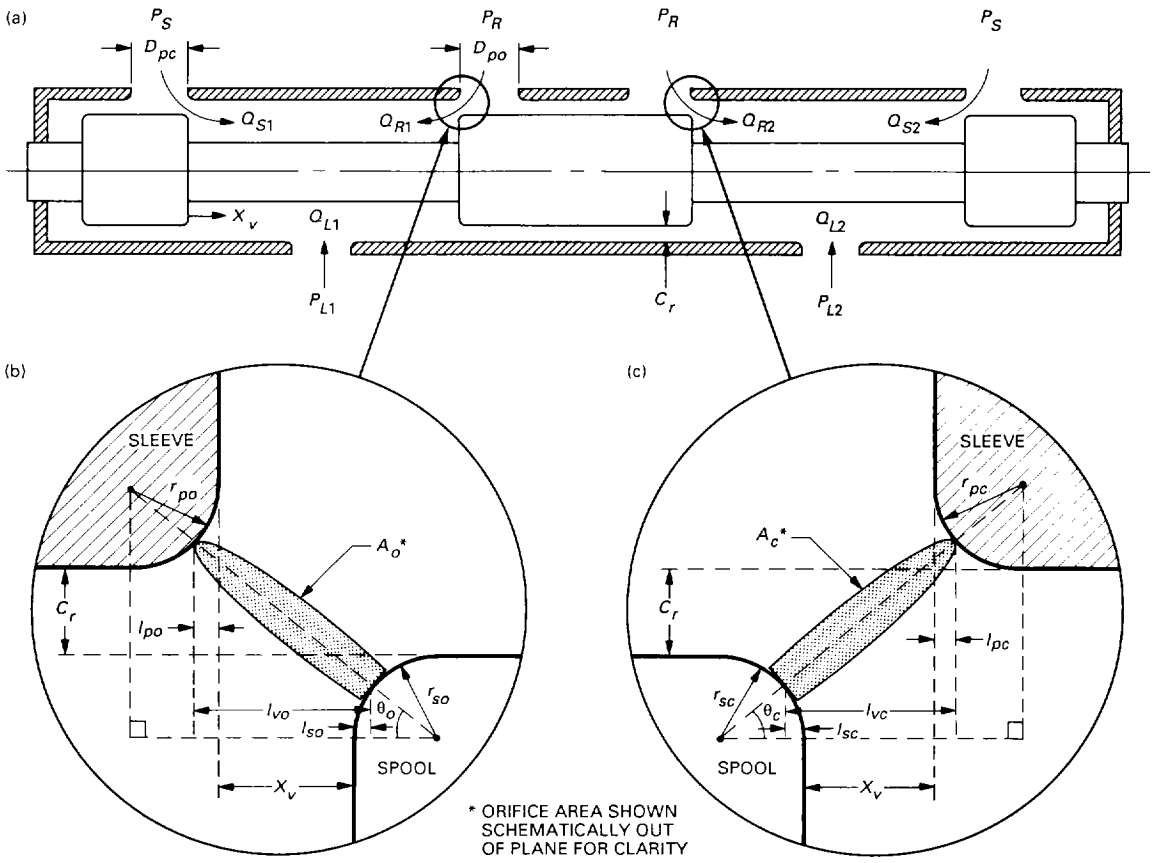

Fig. 1. Valve sleeve and spool assembly cross section: (a) valve at null position, zero spool displacement; (b) opening orifice shown at positive spool displacement; (c) closing orifice shown at negative spool displacement.

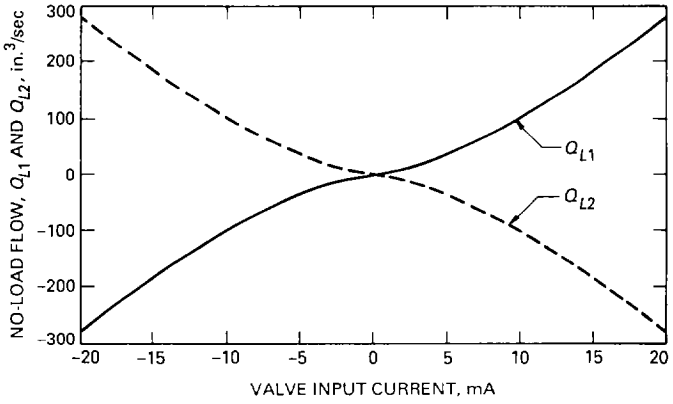

Fig. 2. Valve-flow gain expressed as flow through load ports with no-load or zero differential-load pressure.

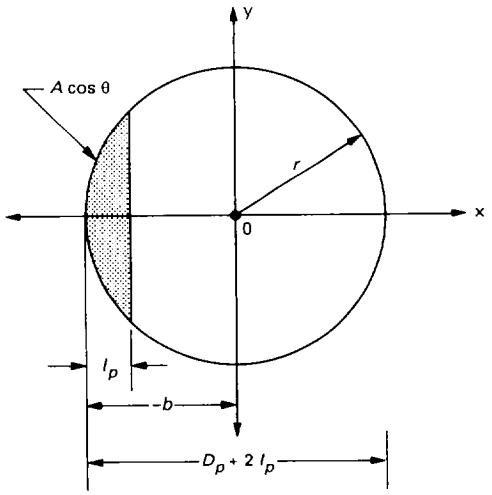

Fig. 4. Integration of semicircle for port-area calculation.

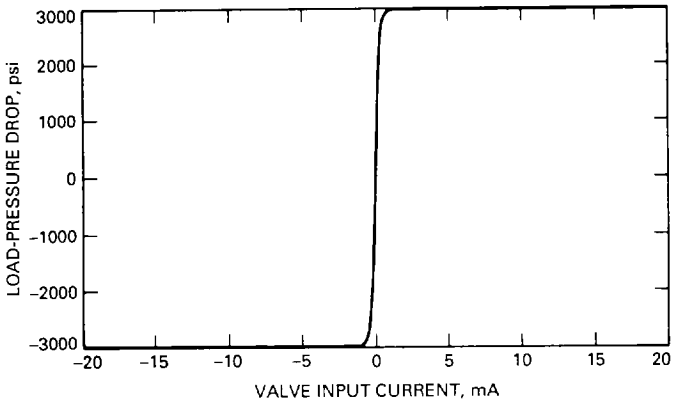

Fig. 3. Valve-pressure gain expressed as the pressure drop across load ports that are blocked to prevent control flow.

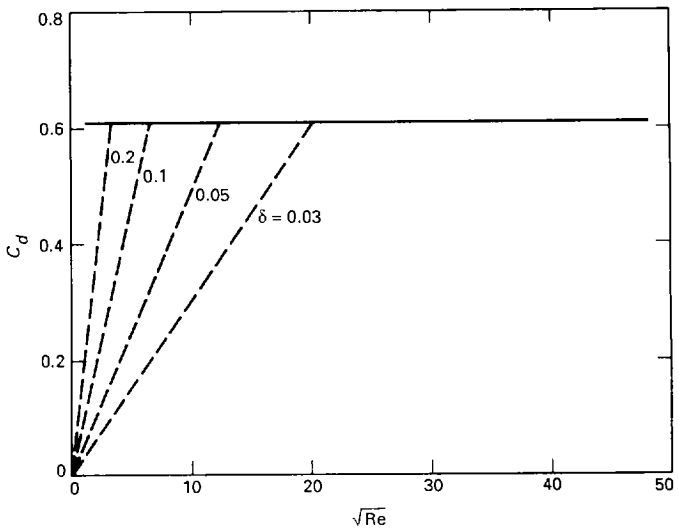

Fig. 5. Asymptotic approximation of discharge coefficient.